



Molecular dynamics simulation of ion separation and water transport through boron nitride nanotubes

Jafar Azamat*, Jaber Jahanbin Sardroodi, Alireza Rastkar

Molecular Simulations Laboratory, Azarbaijan Shahid Madani University, Tabriz, Iran, Tel. +989143118184; Fax: +984124327541; email: jafar.azamat@azaruniv.edu (J. Azamat); Tel./Fax: +984124327541; email: jsardroodi@azaruniv.edu (J. Jahanbin Sardroodi); a_rastkar@azaruniv.edu (A. Rastkar)

Received 7 November 2013; Accepted 2 July 2014

ABSTRACT

Molecular dynamics simulations were performed to investigate ionic selectivity of boron nitride nanotubes. The simulated systems were composed of a boron nitride nanotube inserted in a silicon nitride membrane immersed in an aqueous ionic solution. The considered nanotubes were fixed in a silicon nitride membrane and an external electrical field was applied on the systems along the axis of nanotubes. We found that the (7, 7) and (8, 8) boron nitride nanotubes were exclusively selective to ions. A (7, 7) boron nitride nanotube could selectively conduct Na^+ ions. In contrast, a (8, 8) boron nitride nanotube could selectively conduct Cl^- ions. Some simulated properties, including the ionic current, the water structure inside nanotubes, the retention time of the ions, ion-water radial distribution functions, and normalized transport rate of water with respect to the number of transported ions, were calculated. The current was found to increase linearly with voltage.

Keywords: Desalination; Boron nitride nanotube; Molecular dynamics simulations; PMF

1. Introduction

Selective transport of ions through nanopores is of fundamental interest in a range of physical, chemical, and biological processes. The expansion of effective low-cost water desalination and methods for the removal of ions from water are important from both environmental and economic perspectives. The simplicity of the structure is an advantage for the fabrication devices for desalination. Gating and selectivity are the two most important characteristics of ion separation devices. Ion separation and water transport through nanoscale structures depend on voltage or the binding of molecules. Nanotubes, with their nanoscale

diameters, could lead to potential applications in pharmaceutical and desalination processes.

Boron nitride nanotubes are of importance to the scientific community because of their unique and important properties, making them ideal for structural and electronic applications [1]. A boron nitride nanotube can be imagined as a rolled-up hexagonal BN layer or a carbon nanotube in which alternating B and N atoms are entirely substituted for C atoms. Similar to carbon nanotubes, BNNTs have chirality, an important geometrical parameter, but for them, the chirality does not play an important role in determining the electrical properties [2]. However, the nanoscaled BN with a perfect tubular structure was firstly predicted theoretically only in 1994 [3], and then experimentally synthesized by arc discharge in 1995 [4]. In the

*Corresponding author.

following few years, most works were focused on the synthesis of BNNTs followed by their structural characterizations [5–8].

The behavior of cations and anions in nanopores plays an important role in transport processes in biological and industrial membranes, porous electrodes, and nanomaterials in general. In recent years, there has been increasing attention toward understanding the molecular mechanisms controlling ion transport [9–11]. Recently, a wide variety of nanotubes have been suggested for salt permeation and ion transport [12,13].

To date, researchers have successfully designed and fabricated water and ion-selective nanotubes constructed from carbon [14–23] and boron nitride [20,24–27] atoms. Hilder et al. [21] designed a chloride-selective carbon nanotube with carbonyl ends having chloride conduction. Lee et al. [22] were able to fabricate single-wall carbon nanotubes which were selective to protons.

Here, in order to study the selective transport of sodium and chloride ions through nanotubes, we used boron nitride nanotubes fixed in a silicon-nitride membrane by molecular dynamics simulation method. Molecular dynamics simulation method is the most commonly used and at the same time, the most appropriate tool for the purpose of computer simulation of selectivity of ions. The MD simulation technique can directly investigate the microscopic details of permeation phenomenon. In this work, particular attention has been paid to the number and type of ion permeation from different nanotubes and the dynamical properties of the ions and the solvent molecules. The details of simulation methods are described in Section 2 and our results are discussed in Section 3. Finally, our conclusions are presented in Section 4.

2. Computational method and details

In this work, boron nitride nanotubes with (7, 7) and (8, 8) chirality index were studied. The length of all of nanotubes was approximately 15 Å and their radii were 4.89 and 5.54 Å for (7, 7) and (8, 8) BNNTs, respectively. The considered nanotubes and silicon nitride membrane interacted via both the van der Waals and electrostatic interactions. The electrostatic interactions, due to partial charges on the nanotube and silicon nitride, atoms were the dominant source of the selectivity on the ionic transport in the studied systems. The optimized geometries of the BNNTs were obtained in the B3LYP level of theory with the 6-31G** basis set implemented in GAMESS-US [28]. The value of 1.446 Å, as the optimized B–N bonds distance, was

obtained. The long-range interactions of boron and nitrogen were characterized with the 12-6 Lennard–Jones potential [29,30]. In this work, the parameters for the 12-6 Lennard–Jones potential were $\epsilon_{\text{boron}} = 0.094 \text{ kcal mol}^{-1}$, $\sigma_{\text{boron}} = 3.453 \text{ Å}$, $\epsilon_{\text{nitrogen}} = 0.144 \text{ kcal mol}^{-1}$, and $\sigma_{\text{nitrogen}} = 3.365 \text{ Å}$, respectively. The water–nanotube, water–ion, and ion–nanotube interaction parameters were derived using the Lorentz–Berthelot combining rules. We employed the determined partial charges using density functional theory for BNNTs as presented by Won and Aluru [31].

The molecular dynamics calculations reported here were performed using the NAMD software [32] similar to a previous work [33] with a 1-fs time step and visualized using VMD [34]. In NAMD program, the van der Waals (E_{LJ}) interaction energies are given by:

$$E_{\text{LJ}} = \sqrt{\epsilon_i \epsilon_j} \left[\left(\frac{(\sigma_i + \sigma_j)}{2R_{ij}} \right)^{12} - 2 \left(\frac{(\sigma_i + \sigma_j)}{2R_{ij}} \right)^6 \right] \quad (1)$$

where ϵ_i and σ_i are the usual empirical Lennard–Jones parameters associated with atom i and R_{ij} is the distance between the atoms i and j . Also, all analysis scripts were composed locally using both VMD and Tcl commands. Electrostatic and van der Waals interactions were truncated smoothly by means of a 12-Å spherical cutoff in conjunction with a switching function. The Particle Mesh Ewald algorithm [35] was used for electrostatic calculation with an interpolation function of order five.

The MD domain consisted of a boron nitride nanotube, a silicon-nitride membrane, water, and ions (either sodium or chloride). The system was replicated periodically in all three dimensions. The simulation box for all runs was $35 \times 41 \times 51 \text{ Å}^3$. The energy of the system was first minimized for 0.5 ns, and then equilibrated with molecular dynamics for 4 ns before data collection. We used boron nitride nanotubes with chirality of (7, 7) and (8, 8), fixed in a silicon-nitride membrane immersed in 0.5 M NaCl aqueous solution, as illustrated in Fig. 1.

An electrical field was applied for all considered systems within the whole simulation period. The applied electrical field was represented in internal units of NAMD package, which could be defined by the following equation:

$$e_{\text{field}} = -23.0605492 \frac{V}{l_z} \quad (2)$$

where e_{field} , V , and l_z are the applied electrical field (in $\text{kcal mol}^{-1} \text{ Å}^{-1} \text{ e}^{-1}$), potential difference (in Volt), and

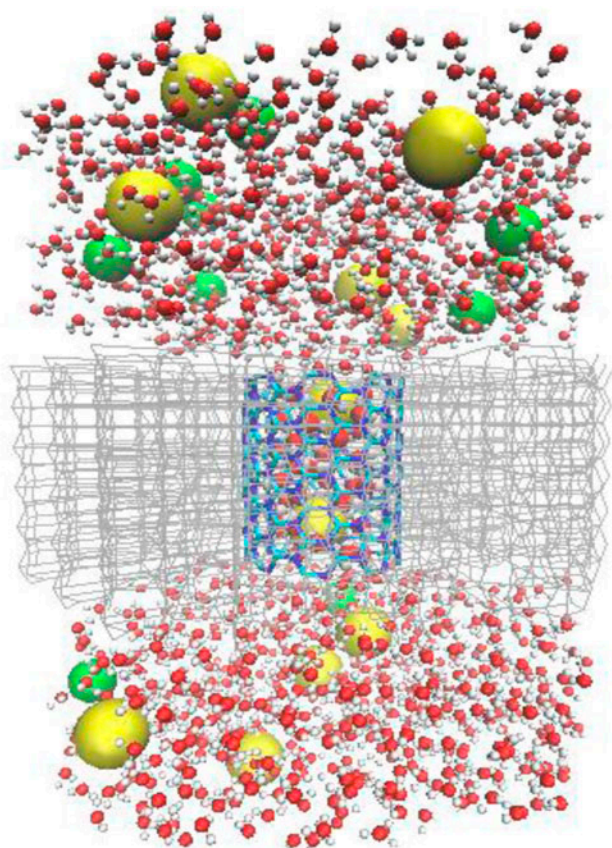


Fig. 1. BNNT (7, 7) shown inside a silicon nitride membrane between two reservoirs containing water and ions.

size of the system along the z -axis (in Angstrom). The system was equilibrated for 0.5 ns to a constant temperature of 298 K and a constant pressure of 1 bar. The Langevin dynamics method, where additional damping and random forces are introduced to maintain an approximately constant temperature across the system, was employed to keep the temperature at 298 K. The pressure was maintained at 1 bar using a Nose–Hoover Langevin piston. The intermolecular three-point potential (TIP3P) model was employed to represent water molecules [36]. This model has been found to be remarkably successful for modeling liquid water under ambient condition and is reasonably successful under other conditions. The empirical CHARMM27 force field [37] was used to describe interatomic interactions for all simulations. For ions, we used the primitive model. The parameters for Na and Cl were obtained from Chandrasekhar et al. [38]. For all runs, the silicon nitride membrane and the BNNT were restrained with a harmonic constraint, while water molecules and ions were allowed to move freely.

The current vs. electric field curve for the studied systems was generated at an ionic concentration of 0.5 M. Current was calculated using the following equation:

$$I = n \cdot q / \Delta t \quad (3)$$

where n , q , and Δt are the average number of ions that cross the nanotube, the charge of the ion, and the simulation time of one run, respectively.

The contrasting ion selectivity of BNNTs can be explained by the potential of mean force (PMF) [39]. The PMF for an ion i , denoted by $W_i(z)$, is computed by integrating the mean force, $\langle F_i(z) \rangle$, which acts on the ion along the nanotube axis, z , due to all other atoms in the system and averaging over all the configurations, i.e.

$$W_i(z) - W_i(z_0) = \int_{z_0}^z \langle F_i(z) \rangle dz \quad (4)$$

where z_0 is the reference position. The mean force distribution was obtained by sampling the force experienced by the ions placed at various positions along the nanotube axis. The PMF of the specific ion moving through the nanotube was determined using umbrella sampling and the data were analyzed using the weighted histogram analysis method [40]. The ion was moved through positions from 0 to 15 Å in 0.5 Å increments and the z component was held using a harmonic constraint of $12.5 \text{ kcal mol}^{-1} \text{ \AA}^{-2}$, whereas the ion was free to move radially. This harmonic constraint was chosen to give enough overlap between each window and its neighbors while constraining the ions to ensure sufficient sampling of the entire reaction coordinate.

3. Results and discussion

In order to obtain ionic current, normalized transport rate of water with respect to the number of transported ions, the retention time of the ions, ion-water radial distribution functions (RDFs), and other parameters, the molecular dynamics simulations were performed.

Water at ambient and biological conditions is a common and important solvent. It is a good solvent for ions and polar molecules and an exceptionally poor solvent for nonpolar or hydrophobic solutes [41,42]. In ice, each water molecule forms four hydrogen bonds, resulting in a rather open network structure. In the liquid under ambient conditions, this

structure persists to some extent, at least within a short range, probably giving water its unique properties. The interaction of ions with water can lead to the breaking of this structure, which is replaced by a different ordering of the molecules in the local field of the ion. Fig. 2 shows the organization of water molecules in the considered nanotubes and RDF nanotube water. It displays that water molecules lie in a cylindrical arrangement inside the nanotubes; also, RDF confirms the structure of water molecules.

Although the considered nanotubes have a radius large enough to accept sodium and chloride ions, our results showed that one Na^+ ion entered the (7, 7) nanotube and was able to travel the entire length of the nanotube and exit it. In contrast, none of the Cl^- ions were able to even enter the (7, 7) nanotube. In the case of (8, 8) nanotube, the opposite phenomenon occurred. This different behavior was governed by dissimilar orientations of dipole moment vector of inner water molecules and the corresponding electrical field inside the nanotubes. The water molecule's dipole moment vector was directed toward the axis of (7, 7) nanotubes and upward of the axis of (8, 8)

nanotubes. These different orientations arose because nitrogen atoms of the membrane surrounded (7, 7) nanotubes and silicon atoms of the membrane surrounded (8, 8) nanotubes.

The thermodynamic basis of the observed designs of ion selectivity was explored by the calculation of potentials of mean force, i.e. of free energy profiles for a given ion as it was moved along the (z) axis of the pore. Fig. 3 includes PMF for the considered systems. It shows that, in a (7, 7) nanotube, there was an energy barrier for Cl^- ions preventing the permeation of Cl^- . In the case of (8, 8) nanotubes, the energy barrier existed for Na^+ ions. In these nanotubes, a deep energy well for ions was produced by the ordered dipole moments of the inner waters. The PMF was computed without any external field. When no electrical field was applied, the ions would enter the nanotube accumulated near the pore center. In the case of

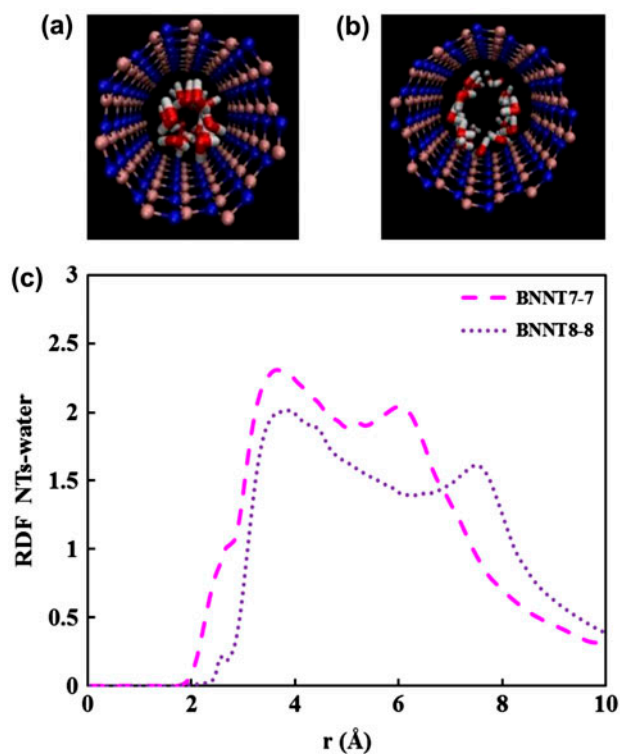


Fig. 2. The position of water molecules inside nanotubes: (a) BNNT (7, 7), (b) BNNT (8, 8) and (c) RDF for nanotube water molecules.

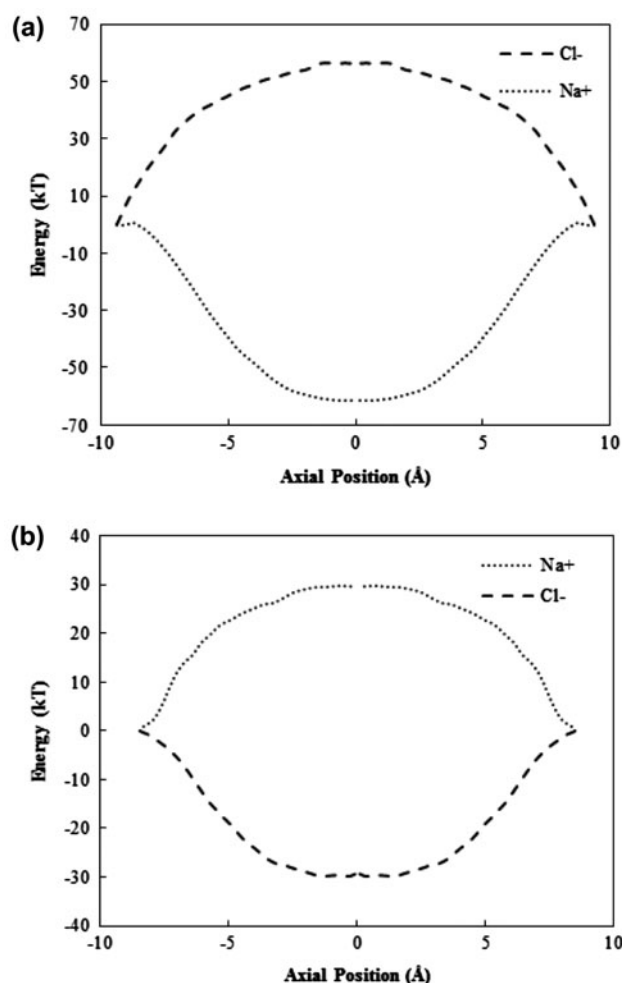


Fig. 3. PMF for ions in: (a) BNNT (7, 7) and (b) BNNT (8, 8).

applying the electrical field, the ions overcame the potential barrier and could exit the nanotube.

PMF shows the variation of free energy function with some degrees of freedom (in our case, the interior coordinates of NT with respect to its center), so no permeation could occur spontaneously when PMF was increased vs. the degree of freedom. In our simulations, the PMF was raised at the pore openings, reaching its maximum value at the pore center inside the nanotube. This was due to the high symmetry of the system and the interactions between anions, nanotubes, and membrane. This was completely in agreement with the results of simulations, thereby showing that the anions could not penetrate the (7, 7) nanotube because PMF had a high free energy barrier.

Fig. 4 displays the current-electrical field profile. The current was shown to increase linearly with the electrical field. This indicated that the number of ions and water molecules passing through the nanotube were increased linearly with the applied electrical field as shown in Fig. 5. By fitting a linear regression to the current-electrical field curve, we obtained sodium conductance of 165.1 pS for the (7, 7) BNNT and chloride conductance of 351.7 pS for the (8, 8) BNNT.

The transport rate of the water through the nanotubes is defined as the ratio of the average number of passing water molecules to the simulation time. Table 1 includes the transport rate of water and Fig. 6 shows the normalized transport rate of water with respect to the number of transported ions. These results showed that the normalized transport rate of water (transported water for one permeated ion) was independent of the applied electrical field.

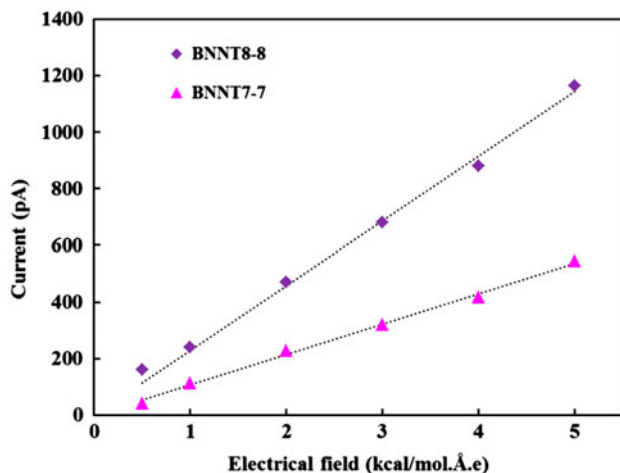


Fig. 4. Current-electrical field curve for Na^+ ion in (7, 7) nanotubes and Cl^- ion in (8, 8) nanotubes; lines have been obtained from a linear regression.

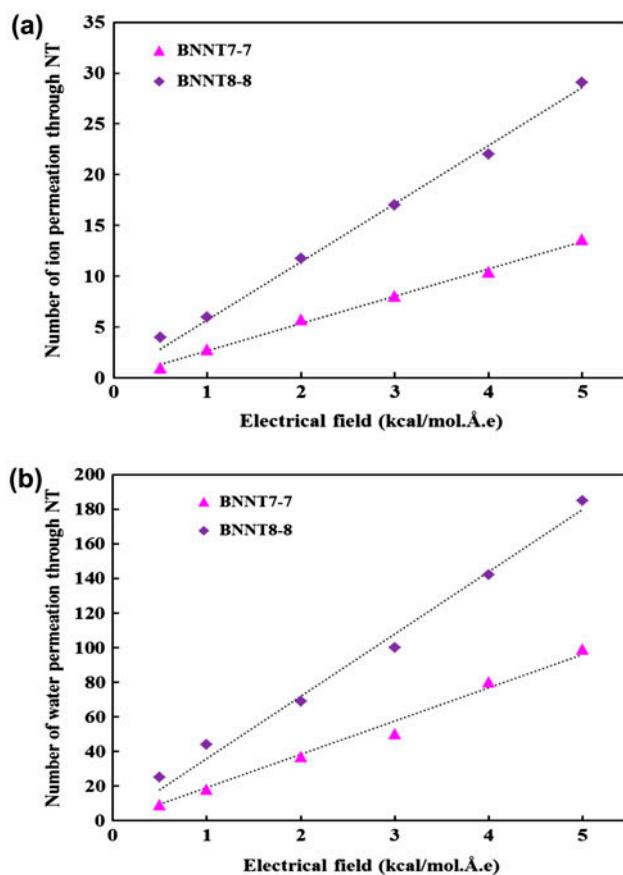


Fig. 5. The number of (a) ions (Na^+ ion in (7, 7) nanotubes and Cl^- ion in (8, 8) nanotubes) and (b) water molecules passing through the nanotubes; lines have been obtained from a linear regression. Each data point represents the average of five sets of simulations.

The water network structure inside the nanotubes was interrupted by the construction of the first hydration shell around the ion inside the nanotube. This caused the reduction in the number of hydrogen bonds between inner waters. The time average of the normalized hydrogen bonds with respect to the number of inner water molecules in different electrical field has been collected in Table 2. As expected, this parameter was increased with increasing the electrical field.

Fig. 7 contains the retention time of the studied systems, i.e. the time of passing one ion through the nanotube as a function of the applied electrical field. This figure shows that the larger the electrical fields, the smaller the retention time. As can be seen, the retention time was larger for (7, 7) boron nitride nanotube.

To describe the structural change of each type of molecule/atom in the simulation cell, the RDF was calculated from trajectories saved during the simulation.

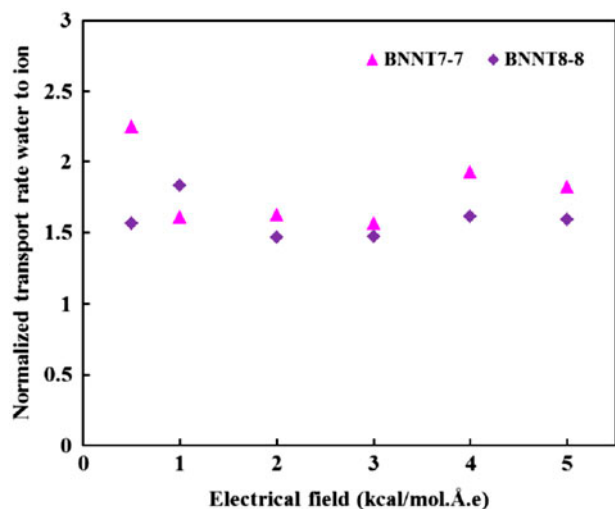


Fig. 6. Normalized transport rate water to ion.

Fig. 8 illustrates the RDF between nanotubes and water molecules. It can be understood that at a short distance (less than atomic diameter), RDF is zero due to the strong repulsive forces. The location of the first maximum and the first minimum was similar in all cases. However, the magnitude of the first peak was different in each case, indicating that the hydration number

(number of water molecules in the first hydration shell of the ion) of the ions was different. In this figure, RDFs for ion-water inside the nanotubes at various electrical fields have been shown. Fig. 8(a) shows Na^+ -water RDF's inside (7, 7) nanotubes, while Fig. 8(b) shows RDFs of Cl^- water inside (8, 8) nanotubes, respectively. One can see that the RDFs varied with the values of electrical fields. These variations can be explained based on the retention times of the ions. At lower electrical fields, ions spend more time inside the hydration shell through nanotubes; in other words, they had a larger retention time and therefore, the RDFs would be intensified. A close examination of Figs. 7 and 8 reveals that the RDF for considered nanotubes was of the same order of magnitude as that of the retention times. This means that the RDF with higher peak corresponded to a larger retention time or a lower electrical field.

Fig. 9(a) and (b) show the z positions of the ions at each simulation time. These figures show that there was an overlap between the retention times of ions for lower electrical field; however, for the higher electrical fields, this overlap did not exist. This means that in the case of lower electric field, one ion could enter the nanotube and would not exit until a second ion entered, but at the higher electric field, ions permeated without any assistance from other ions.

Table 1
Transport rate for water molecules

Electrical field (kcal mol ⁻¹ Å ⁻¹ e ⁻¹)	BNNT (7, 7)		BNNT (8, 8)	
	Water permeation	Transport rate	Water permeation	Transport rate
0.5	9	2.25	25	6.25
1	18	4.5	44	11
2	37	9.25	69	17.25
3	50	12.5	100	25
4	80	20	142	35.5
5	99	24.75	185	46.25

Table 2
The time average of the normalized hydrogen bonds with respect to the number of inner water molecules

Electrical field (kcal mol ⁻¹ Å ⁻¹ e ⁻¹)	BNNT (7, 7)	BNNT (8, 8)
0.5	0.206	0.555
1	0.209	0.639
2	0.372	0.741
3	0.464	0.818
4	0.553	0.852
5	0.671	0.869

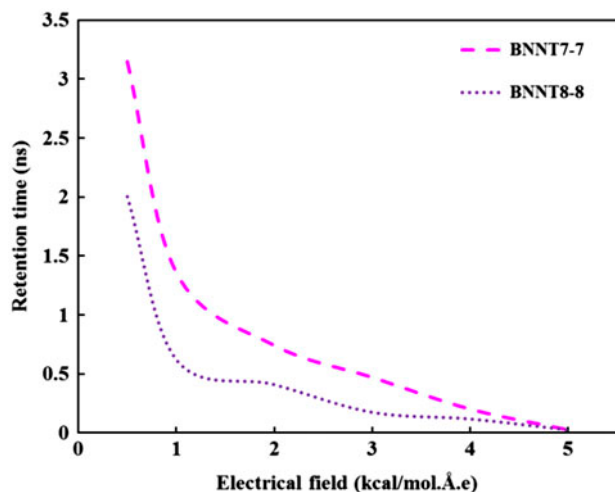


Fig. 7. Retention time of ions for each applied electrical field: Na^+ in nanotubes (7, 7) and Cl^- in nanotubes (8, 8).

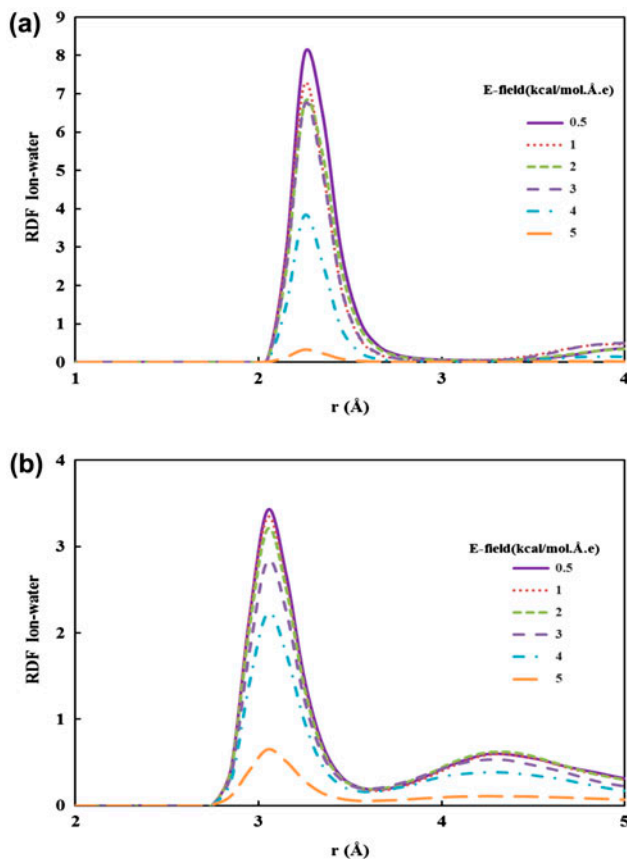


Fig. 8. RDF for ion-water inside the nanotubes at various electrical field: (a) BNNT (7, 7) and (b) BNNT (8, 8).

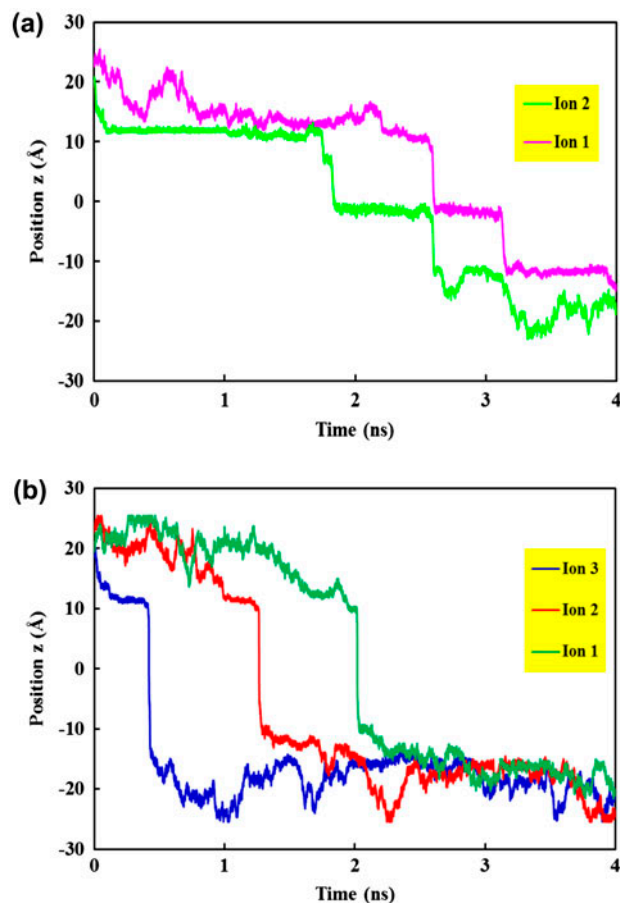


Fig. 9. The z positions of the ions at each simulation time for: (a) lower electrical field for BNNT (7, 7) and (b) higher electrical field for BNNT (7, 7).

4. Conclusion

The expansion of effective low-cost water desalination and methods for the removal of ions from water are important from both environmental and economic perspectives. In this work, we used boron nitride nanotubes for this purpose. The simplicity of the structure was an advantage for the fabrication devices for the desalination. Molecular dynamics simulations were carried out to study the selectivity mechanism of nanopores by studying the ion permeation through (7, 7) and (8, 8) boron nitride nanotubes. It was shown that the ion permeation through nanotubes fixed in a silicon nitride membrane happened in the presence of electrical field and it was selective. Our results showed that one Na^+ ion entered the (7, 7) BNNT and was able to travel the entire length of the nanotube and exit it. In contrast, none of the Cl^- ions were able to even enter the (7, 7) nanotube. In the case of (8, 8) BNNT, the opposite phenomenon occurred. Unlike

carbon nanotubes, this effect was achieved without the need to functionalize the nanotube surface. This simplicity in structure represented a significant advantage for manufacturing an ion-selective nanodevice. Some of the simulated properties including the ionic current, retention time, transport rate of water, and ion-water RDFs were influenced by the applied electrical field. The variation of ionic current with respect to electrical field was linear.

Acknowledgment

Authors thank the Azarbaijan Shahid Madani University and Iranian Nanotechnology Initiative Council for their support.

References

- [1] D. Golberg, Y. Bando, C.C. Tang, C.Y. Zhi, Boron nitride nanotubes, *Adv. Mater.* 19 (2007) 2413–2432.
- [2] B. Akdim, R. Pachter, X. Duan, W.W. Adams, Comparative theoretical study of single-wall carbon and boron-nitride nanotubes, *Phys. Rev. B* 67 (2003) 245404.
- [3] A. Rubio, J.L. Corkill, M.L. Cohen, Theory of graphitic boron nitride nanotubes, *Phys. Rev. B* 49 (1994) 5081–5084.
- [4] N.G. Chopra, R.J. Luyken, K. Cherrey, V.H. Crespi, M.L. Cohen, S.G. Louie, A. Zettl, Boron nitride nanotubes, *Science* 269 (1995) 966–967.
- [5] D. Golberg, Y. Bando, M. Eremets, K. Takemura, K. Kurashima, H. Yusa, Nanotubes in boron nitride laser heated at high pressure, *Appl. Phys. Lett.* 69 (1996) 2045–2047.
- [6] O.R. Lourie, C.R. Jones, B.M. Bartlett, P.C. Gibbons, R.S. Ruoff, W.E. Buhro, CVD growth of boron nitride nanotubes, *Chem. Mater.* 12 (2000) 1808–1810.
- [7] Y. Chen, J.F. Gerald, Mechanochemical synthesis of boron nitride nanotubes, *Mater. Sci. Forum* 312–314 (1999) 173–178.
- [8] W. Han, Y. Bando, K. Kurashima, T. Sato, Synthesis of boron nitride nanotubes from carbon nanotubes by a substitution reaction, *Appl. Phys. Lett.* 73 (1998) 3085–3087.
- [9] T. Lu, A.Y. Ting, J. Mainland, L.Y. Jan, P.G. Schultz, J. Yang, Probing ion permeation and gating in a K^+ channel with backbone mutations in the selectivity filter, *Nat. Neurosci.* 4 (2001) 239–246.
- [10] J. Åqvist, V. Luzhkov, Ion permeation mechanism of the potassium channel, *Nature* 404 (2000) 881–884.
- [11] D.A. Doyle, J.M. Cabral, R.A. Pfuetzner, A. Kuo, J.M. Gulbis, S.L. Cohen, B.T. Chait, R. MacKinnon, The structure of the potassium channel: Molecular basis of K^+ conduction and selectivity, *Science* 280 (1998) 69–77.
- [12] D. Stein, M. Kruithof, C. Dekker, Surface-charge-governed ion transport in nanofluidic channels, *Phys. Rev. Lett.* 93 (2004) 035901.
- [13] K. Leung, S.B. Rempe, C.D. Lorenz, Salt permeation and exclusion in hydroxylated and functionalized silica pores, *Phys. Rev. Lett.* 96 (2006) 095504.
- [14] A. Kalra, S. Garde, G. Hummer, Osmotic water transport through carbon nanotube membranes, *Proc. Nat. Acad. Sci.* 100 (2003) 10175–10180.
- [15] A. Waghe, J.C. Rasaiah, G. Hummer, Filling and emptying kinetics of carbon nanotubes in water, *J. Chem. Phys.* 117 (2002) 10789–10795.
- [16] C.F. Lopez, S.O. Nielsen, P.B. Moore, M.L. Klein, Understanding nature's design for a nanosyringe, *Proc. Nat. Acad. Sci.* 101 (2004) 4431–4434.
- [17] M. Majumder, N. Chopra, R. Andrews, B.J. Hinds, Nanoscale hydrodynamics: Enhanced flow in carbon nanotubes, *Nature* 438 (2005) 44–44.
- [18] F. Fornasiero, H.G. Park, J.K. Holt, M. Stadermann, C.P. Grigoropoulos, A. Noy, O. Bakajin, Ion exclusion by sub-2-nm carbon nanotube pores, *Proc. Nat. Acad. Sci.* 105 (2008) 17250–17255.
- [19] B. Corry, Designing carbon nanotube membranes for efficient water desalination, *J. Phys. Chem. B* 112 (2008) 1427–1434.
- [20] M.E. Suk, A.V. Raghunathan, N.R. Aluru, Fast reverse osmosis using boron nitride and carbon nanotubes, *Appl. Phys. Lett.* 92 (2008) 133120–133122.
- [21] T.A. Hilder, D. Gordon, S.-H. Chung, Synthetic chloride-selective carbon nanotubes examined by using molecular and stochastic dynamics, *Biophys. J.* 99 (2010) 1734–1742.
- [22] C.Y. Lee, W. Choi, J.-H. Han, M.S. Strano, Coherence resonance in a single-walled carbon nanotube ion channel, *Science* 329 (2010) 1320–1324.
- [23] B. Corry, Water and ion transport through functionalised carbon nanotubes: Implications for desalination technology, *Energy. Environ. Sci.* 4 (2011) 751–759.
- [24] C.Y. Won, N.R. Aluru, A chloride ion-selective boron nitride nanotube, *Chem. Phys. Lett.* 478 (2009) 185–190.
- [25] W. Lei, D. Portehault, D. Liu, S. Qin, Y. Chen, Porous boron nitride nanosheets for effective water cleaning, *Nat. Commun.* 4 (2013) 1777–1784.
- [26] T.A. Hilder, D. Gordon, S.-H. Chung, Salt rejection and water transport through boron nitride nanotubes, *Small* 5 (2009) 2183–2190.
- [27] S. Ebrahimi-Nejad, A. Shokuhfar, Compressive buckling of open-ended boron nitride nanotubes in hydrogen storage applications, *Phys. E* 50 (2013) 29–36.
- [28] M.W. Schmidt, K.K. Baldrige, J.A. Boatz, S.T. Elbert, M.S. Gordon, J.H. Jensen, S. Koseki, N. Matsunaga, K.A. Nguyen, S. Su, T.L. Windus, M. Dupuis, J.A. Montgomery, General atomic and molecular electronic structure system, *J. Comput. Chem.* 14 (1993) 1347–1363.
- [29] R.J. Mashl, S. Joseph, N.R. Aluru, E. Jakobsson, Anomalous immobilized water: A new water phase induced by confinement in nanotubes, *Nano Lett.* 3 (2003) 589–592.
- [30] C.Y. Won, N.R. Aluru, Water permeation through a subnanometer boron nitride nanotube, *J. Am. Chem. Soc.* 129 (2007) 2748–2749.
- [31] C.Y. Won, N.R. Aluru, Structure and dynamics of water confined in a boron nitride nanotube, *J. Phys. Chem. C* 112 (2008) 1812–1818.

- [32] L. Kalé, R. Skeel, M. Bhandarkar, R. Brunner, A. Gursoy, N. Krawetz, J. Phillips, A. Shinozaki, K. Varadarajan, K. Schulten, NAMD2: Greater scalability for parallel molecular dynamics, *J. Comput. Phys.* 151 (1999) 283–312.
- [33] J.J. Sardroodi, J. Azamat, A. Rastkar, N.R. Yousefnia, The preferential permeation of ions across carbon and boron nitride nanotubes, *Chem. Phys.* 403 (2012) 105–112.
- [34] W. Humphrey, A. Dalke, K. Schulten, VMD: Visual molecular dynamics, *J. Mol. Graphics* 14 (1996) 33–38.
- [35] T. Darden, D. York, L. Pedersen, Particle mesh Ewald: An $N \cdot \log(N)$ method for Ewald sums in large systems, *J. Chem. Phys.* 98 (1993) 10089–10092.
- [36] W.L. Jorgensen, J. Chandrasekhar, J.D. Madura, R.W. Impey, M.L. Klein, Comparison of simple potential functions for simulating liquid water, *J. Chem. Phys.* 79 (1983) 926–935.
- [37] A.D. MacKerell, D. Bashford, M. Bellott, R.L. Dunbrack, J.D. Evanseck, M.J. Field, S. Fischer, J. Gao, H. Guo, S. Ha, D. Joseph-McCarthy, L. Kuchnir, K. Kuczera, F. T. K. Lau, C. Mattos, S. Michnick, T. Ngo, D.T. Nguyen, B. Prodhom, W.E. Reiher, B. Roux, M. Schlenkrich, J.C. Smith, R. Stote, J. Straub, M. Watanabe, J. Wiórkiewicz-Kuczera, D. Yin, M. Karplus, All-atom empirical potential for molecular modeling and dynamics studies of proteins, *J. Phys. Chem. B* 102 (1998) 3586–3616.
- [38] J. Chandrasekhar, D.C. Spellmeyer, W.L. Jorgensen, Energy component analysis for dilute aqueous solutions of lithium(1+), sodium(1+), fluoride(1-), and chloride(1-) ions, *J. Am. Chem. Soc.* 106 (1984) 903–910.
- [39] R. Kjellander, H. Greberg, Mechanisms behind concentration profiles illustrated by charge and concentration distributions around ions in double layers, *J. Electroanal. Chem.* 450 (1998) 233–251.
- [40] A. Grossfield, WHAM: The Weighted Histogram Analysis Method, 2014, Version 2.0.8. Available from: <http://membrane.urmc.rochester.edu/content/wham>.
- [41] F. Franks, Water, A Comprehensive Treatise, Plenum Press, New York, NY, 1972.
- [42] D.S. Eisenberg, W. Kauzmann, The Structure and Properties of Water, Oxford University Press, Oxford, NY, 2005.